

Figure 6-1 Proposed e-beam direct patterning process.

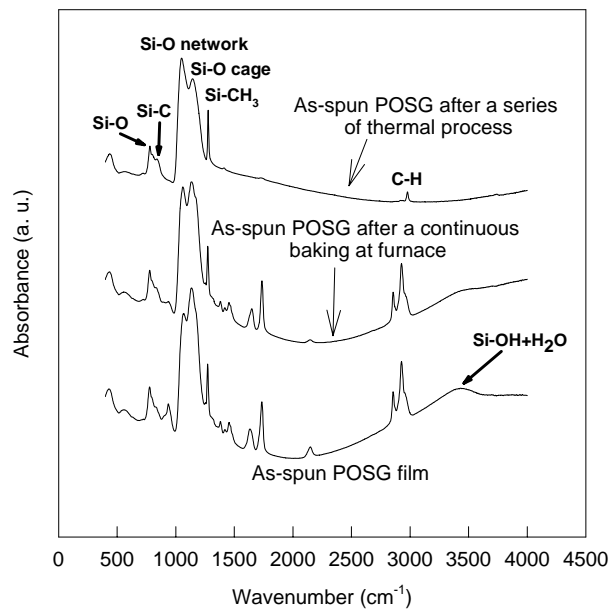


Figure 6-2 The FTIR spectra of as-spun POSG film after a series of bake and furnace curing steps

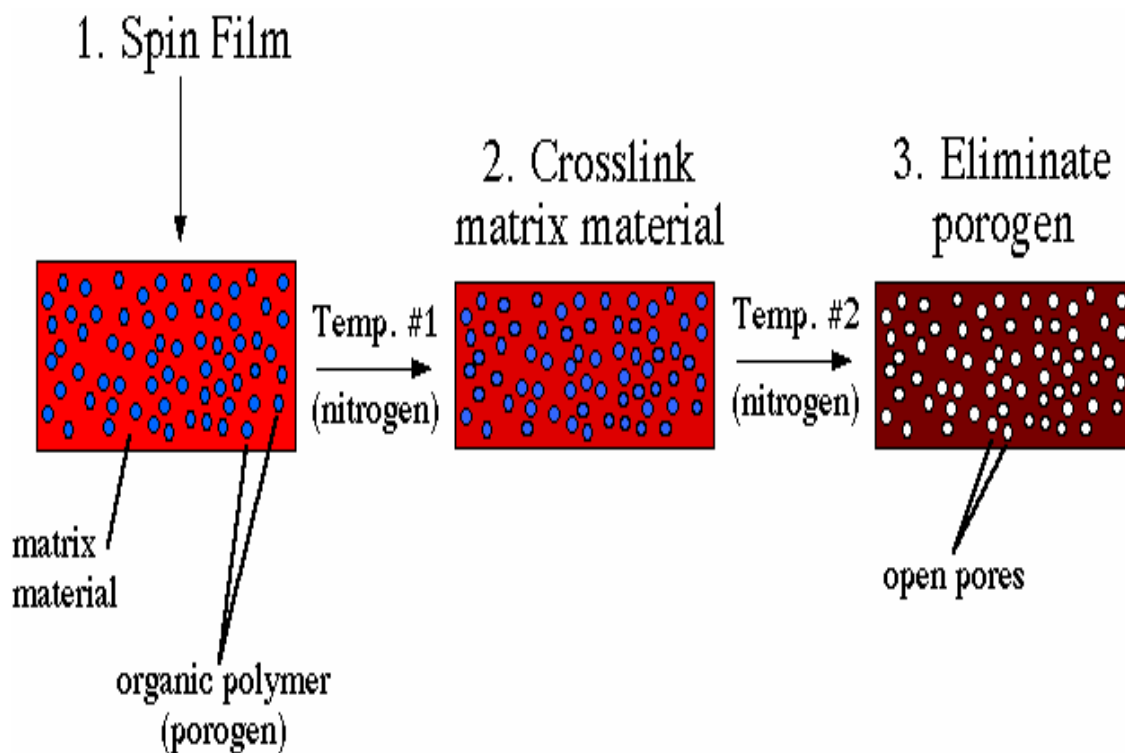


Figure 6-3 The brief diagram of POSG formation procedures.

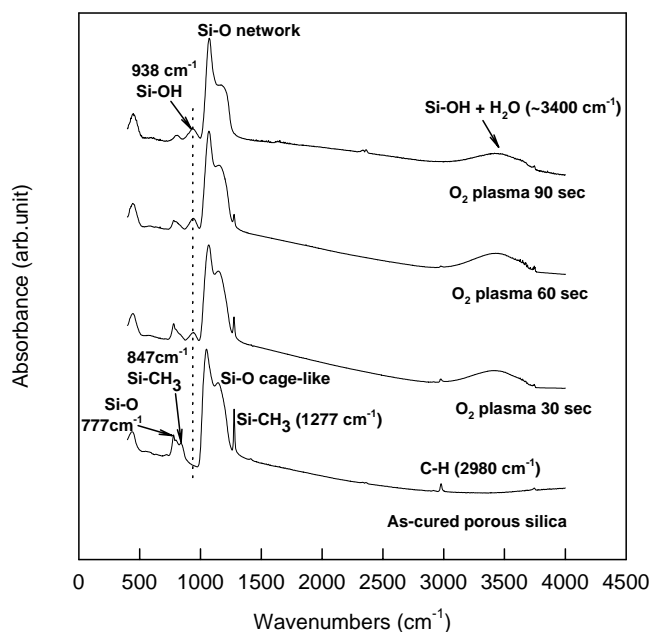
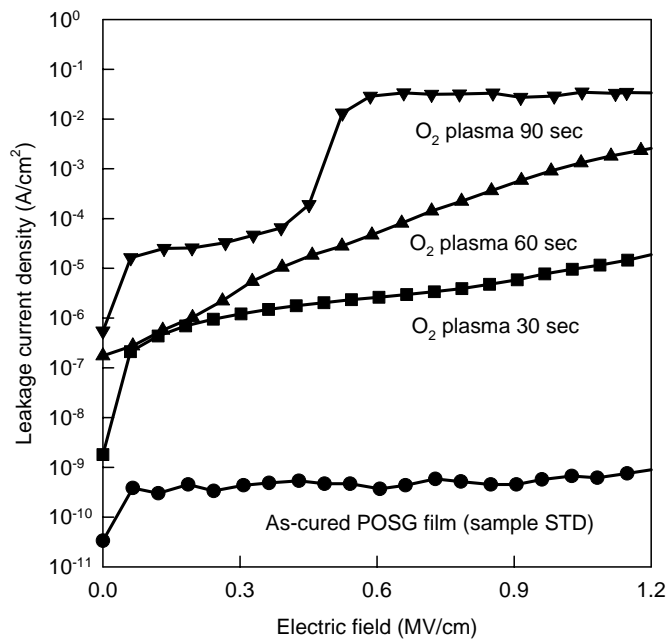
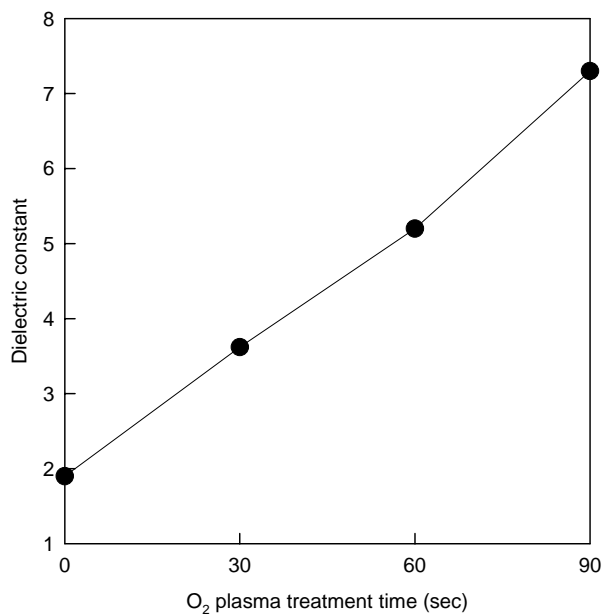


Figure 6-4 FTIR spectra of POSG films after O₂ plasma ashing for 30 to 90 sec.



(a)



(b)

Figure 6-5 Dielectric properties of POSG after O₂ plasma ashing for 30 to 90 sec (a) leakage current density of POSG films versus electric field (b) dielectric constant of post-treated POSG films.

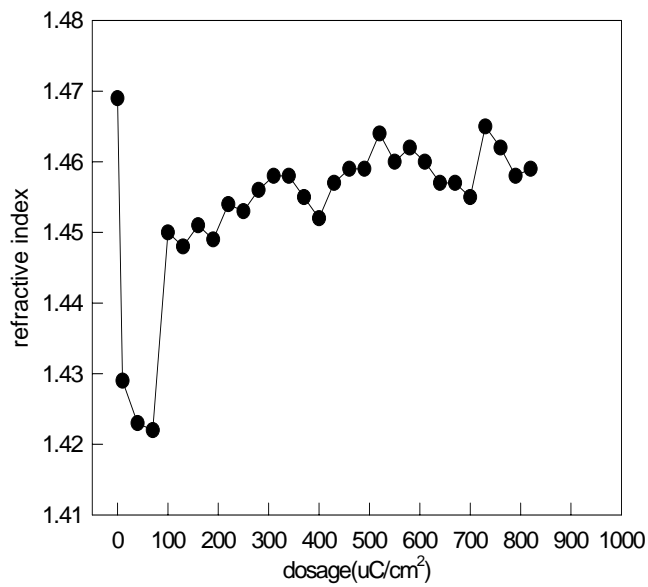


Figure 6-6 The variation of refractive index of POSG films with electron exposed doses from 2 uC/cm² to 810 uC/cm².

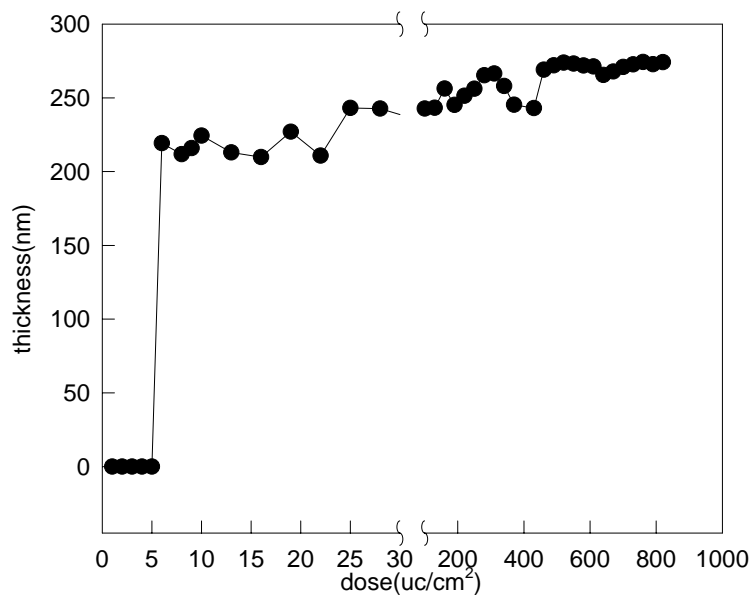


Figure 6-7 The remained thickness of the POSG film with different doses after development.

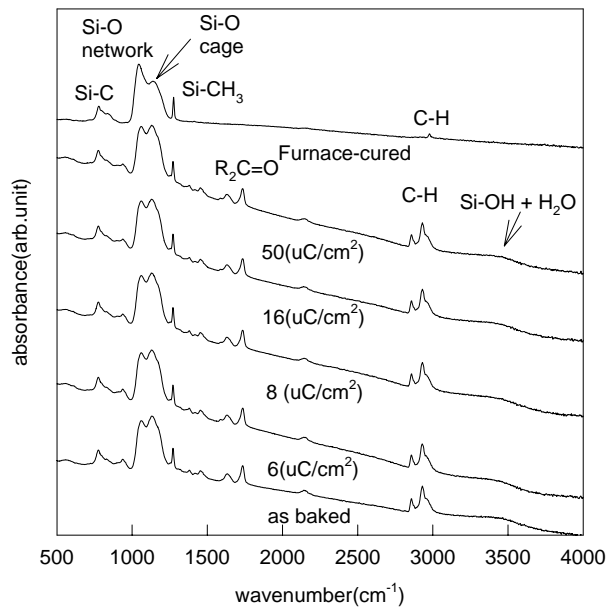


Figure 6-8 FTIR spectra of POSG films with different doses of electron beam exposure.

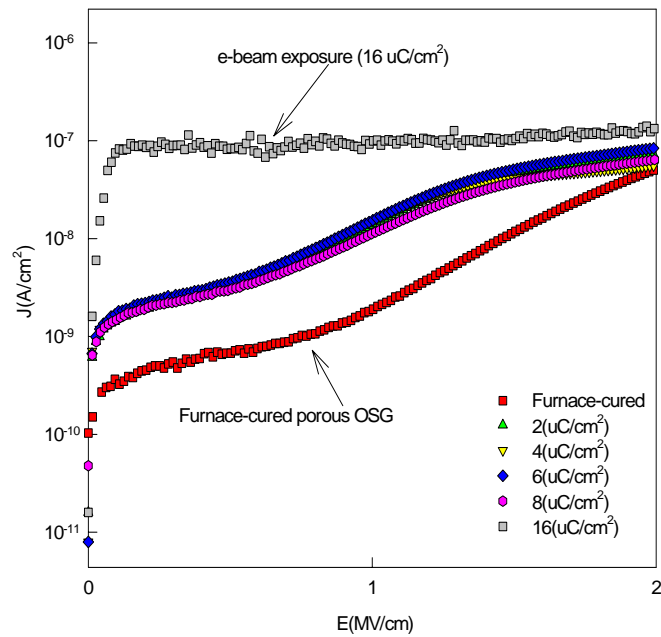


Figure 6-9 The leakage current densities of e-beam exposed POSG films at different doses.

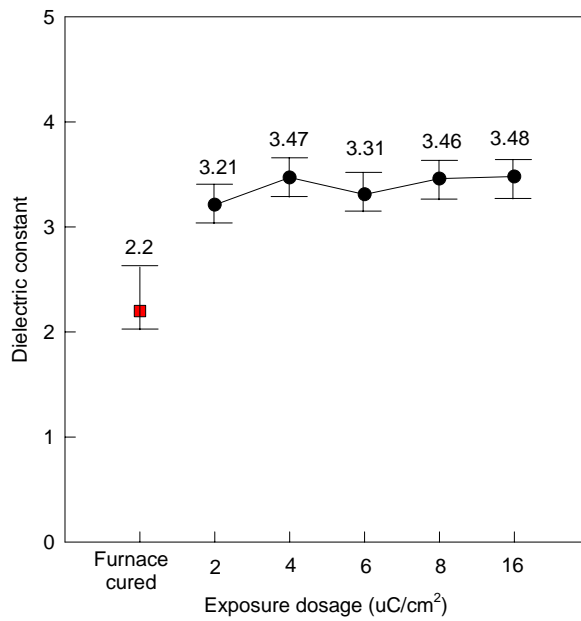


Figure 6-10 Dielectric constant of e-beam exposed POSG films at different doses

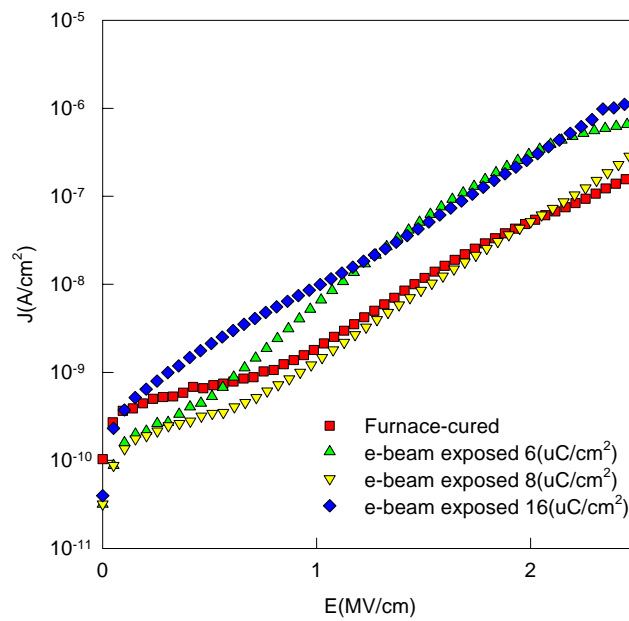


Figure 6-11 The leakage current densities of e-beam exposed POSG films at different doses with furnace annealing process.

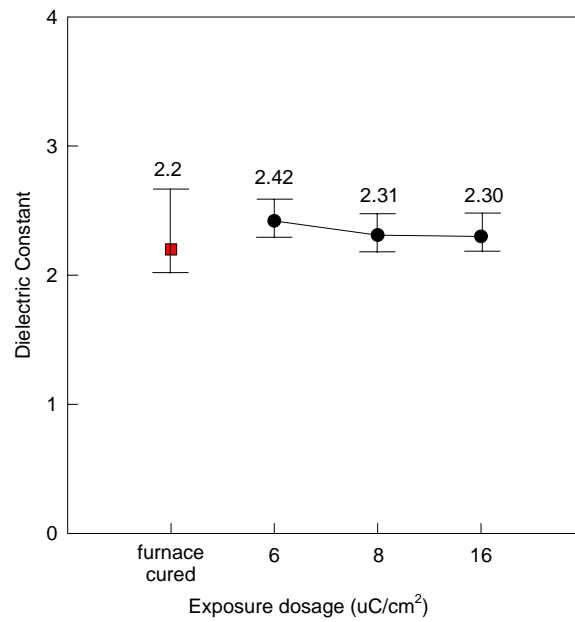


Figure 6-12 The dielectric constant of e-beam exposed POSG films at different doses with furnace annealing process.

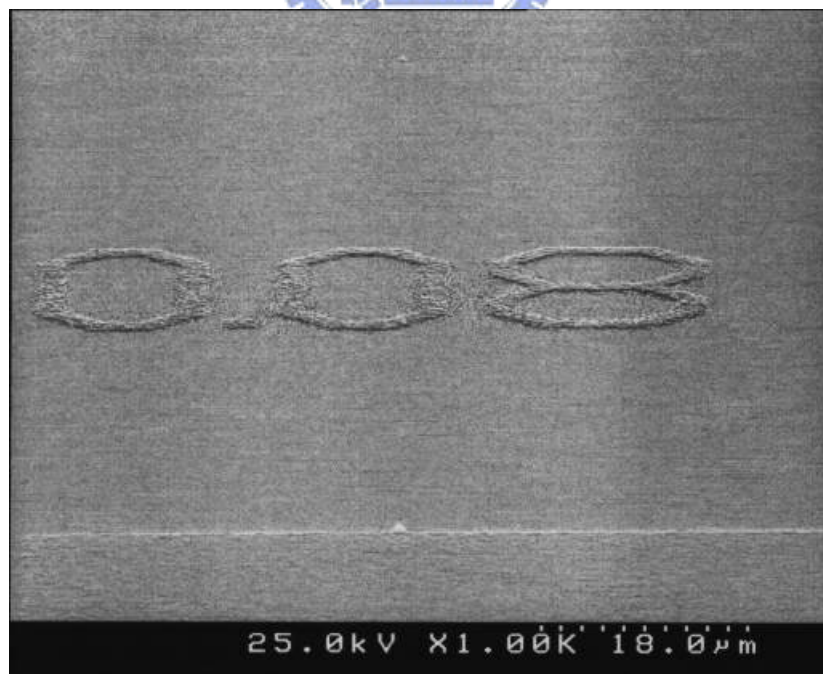


Figure 6-13 The SEM image of patterned wafer after e-beam curing and development processes without post-exposure annealing.

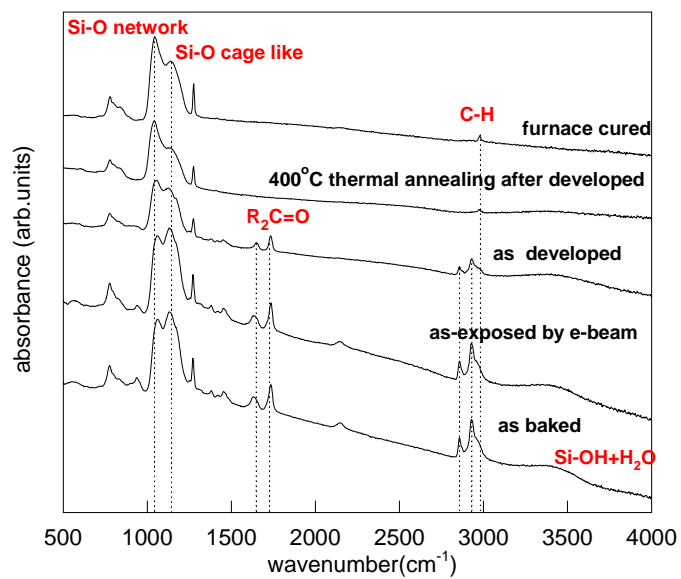
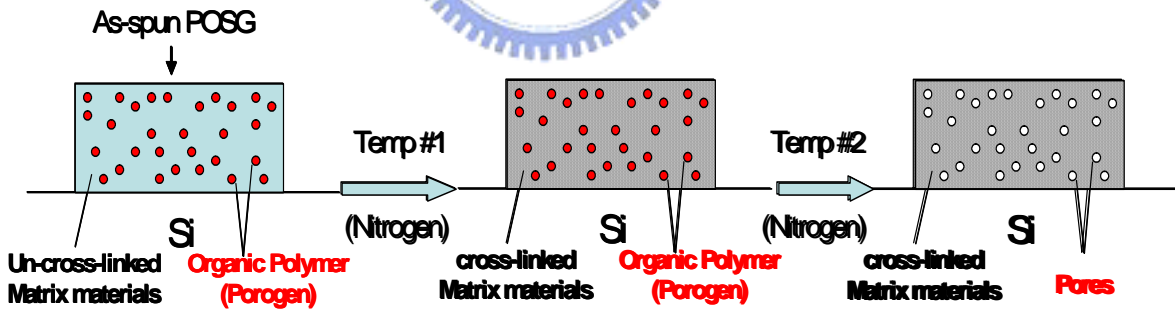
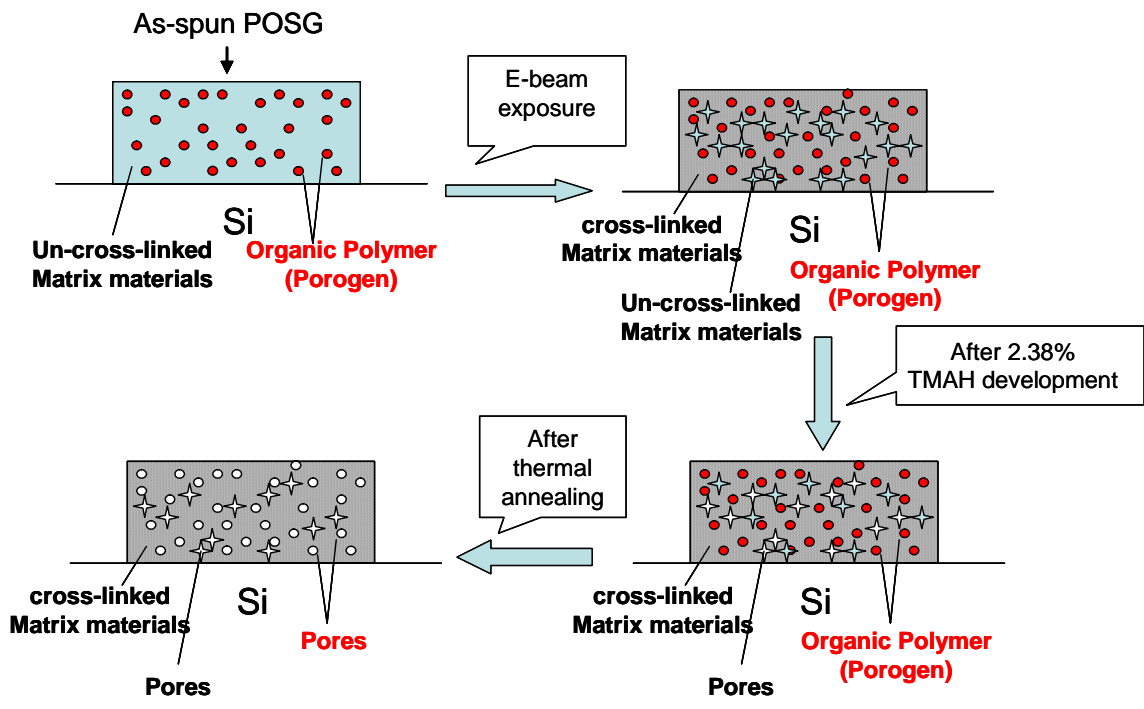


Figure 6-14 The FTIR spectra of POSG films with e-beam exposure and followed by development and post-thermal annealing treatments.



(b)

Figure 6-15 The proposed model for the decrease of dielectric constant on the e-beam exposed POSG after development and subsequent thermal annealing processes (a) e-beam direct patterning process (b) traditional furnace curing process

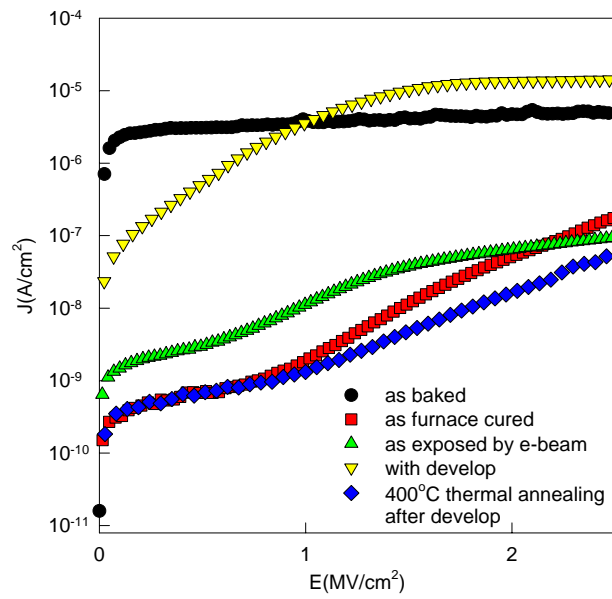


Figure 6-16 The leakage current density of e-beam exposed POSG films with 8 $\mu\text{C}/\text{cm}^2$ dosage after undergoing various treatment.

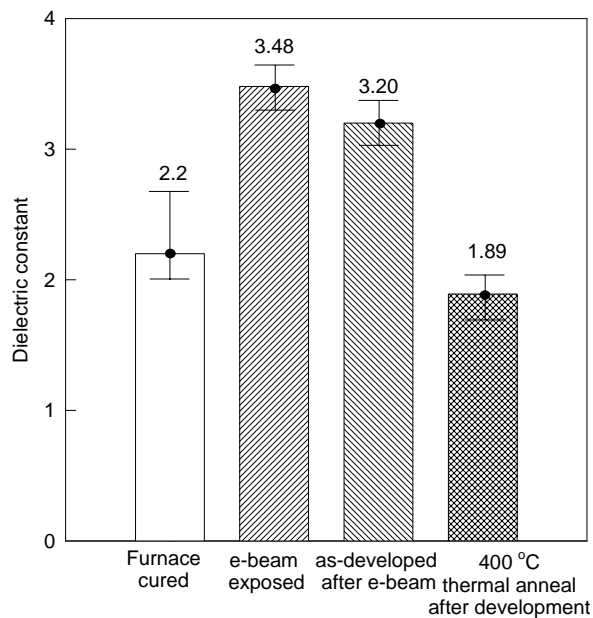


Figure 6-17 The dielectric constant of e-beam exposed POSG films with 8 $\mu\text{C}/\text{cm}^2$ dosage after undergoing various treatment.

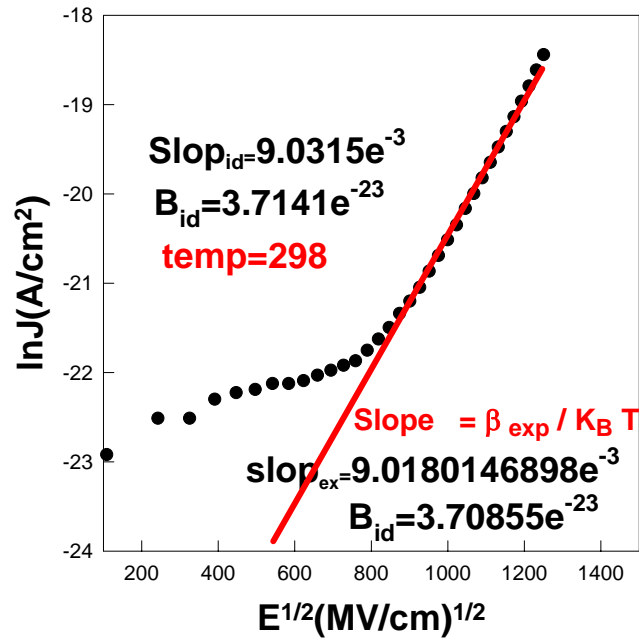


Figure 6-18 The leakage current behavior of furnace cured POSG film.

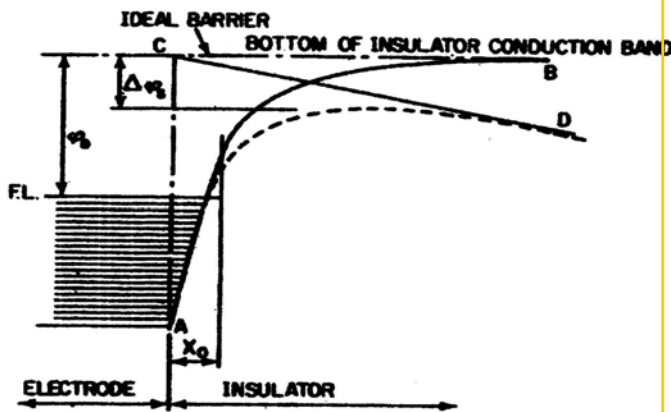


Image-force lowering of a metal-vacuum barrier.

This potential energy for an electron, $-q\psi(x)$.

Curve B : without external field

Curve D : with an external field

😊 No external field :

$$F_{\text{Image Force}} = -qE = -\frac{q^2}{4\pi\epsilon_0(2x)^2}$$

$$-\psi(x) = -\frac{1}{q} \int_x^\infty F_{\text{Image Force}} dx$$

$$= -\frac{q}{16\pi\epsilon_0 x}$$

😊 When an external field E_{ext} is applied:

$$-\psi(x) = -\frac{q}{16\pi\epsilon_0 x} - E_{\text{ext}}x$$

$$x_0 = \left(\frac{q}{16\pi\epsilon_0 E_{\text{ext}}}\right)^{1/2}$$

$$\Delta\phi = \left(\frac{qE_{\text{ext}}}{4\pi\epsilon_0}\right)^{1/2}$$

Figure 6-19 The band diagram of schottky emission mechanism for a metal/furnace-cured POSG/Si capacitor.

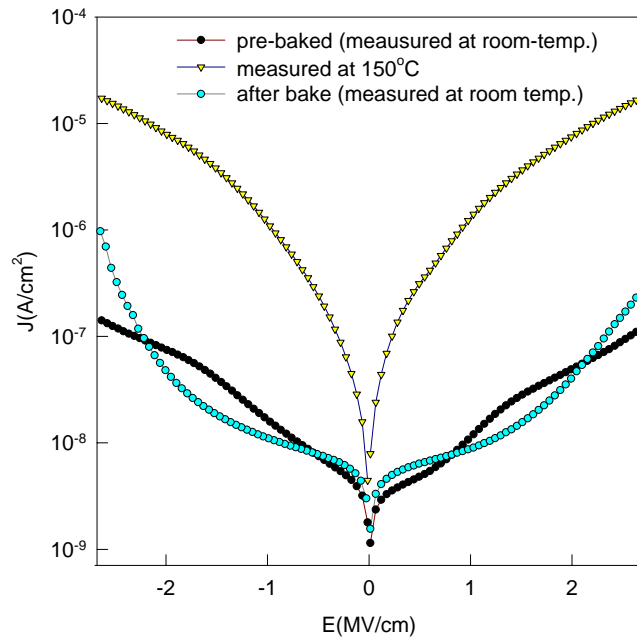


Figure 6-20 The leakage current density of e-beam exposed POSG film measured at different temperature.

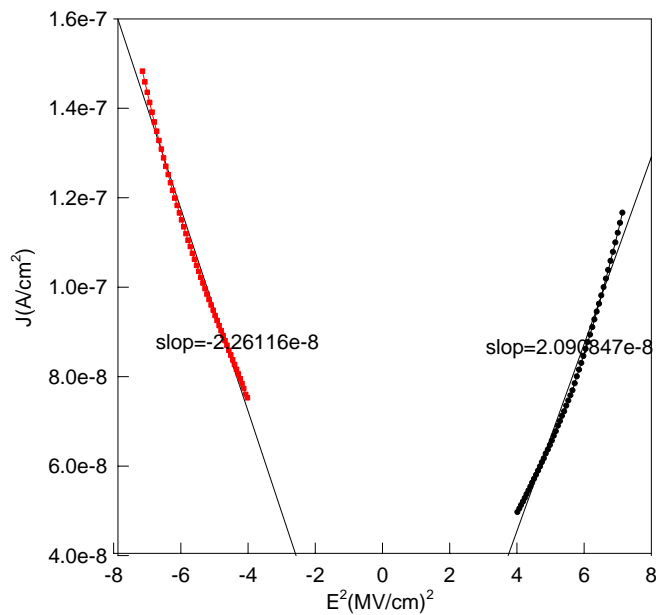


Figure 6-21 The current fitting of e-beam exposed POSG film at room temperature.

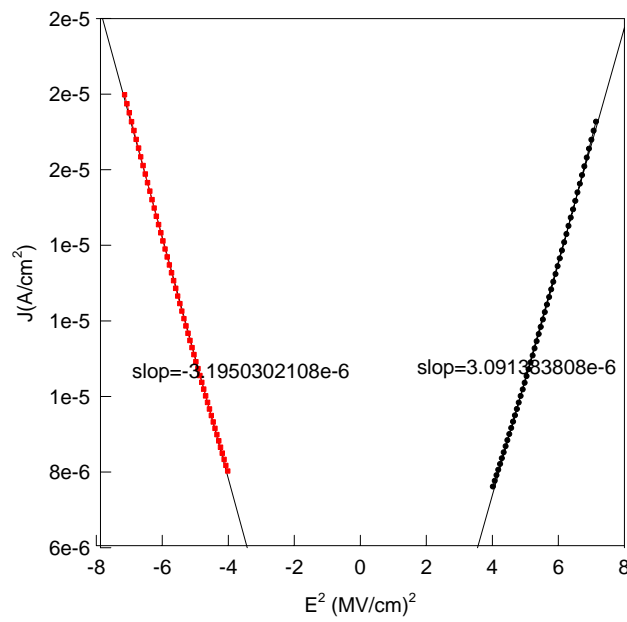


Figure 6-22 The current fitting of e-beam exposed POSG film at 150 °C.

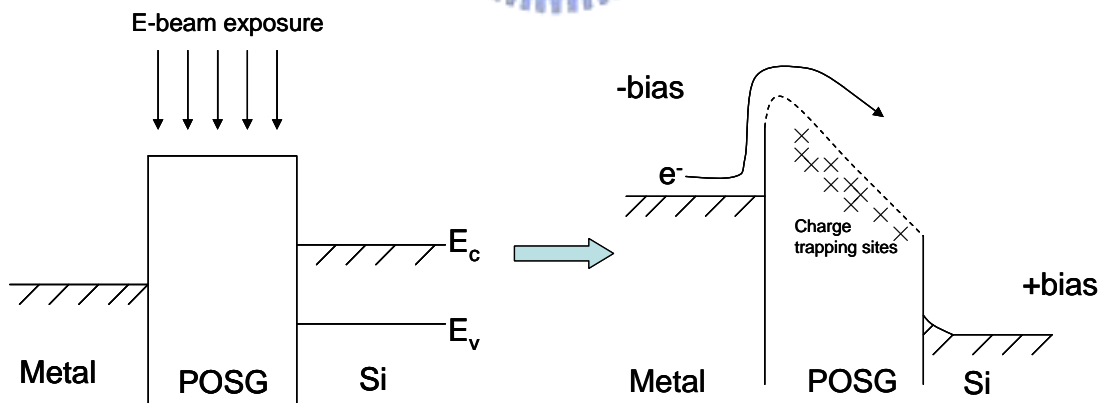


Figure 6-23 The band diagram of space charge limit current mechanisms for e-beam exposed POSG MIS structure.